



Compressive behavior of MWCNT/epoxy composite mats

Konstantinos G. Dassios^{a,b,*}, Simone Musso^c, Costas Galiotis^{a,d}

^a Department of Materials Science and Engineering, University of Ioannina, Ioannina 45110, Greece

^b Foundation for Research and Technology Hellas, Institute of Chemical Engineering and High Temperature Processes, Stadiou Street, Platani, Patras GR-26504, Greece

^c Massachusetts Institute of Technology, Department of Civil and Environmental Engineering, 77 Massachusetts Avenue, Cambridge, MA 02139, United States

^d Department of Materials Science, University of Patras, Rio GR-26500, Greece

ARTICLE INFO

Article history:

Received 10 November 2011

Received in revised form 14 March 2012

Accepted 18 March 2012

Available online 24 March 2012

Keywords:

- A. Carbon nanotubes
- A. Nanocomposites
- B. Mechanical properties
- D. Scanning Electron Microscopy (SEM)
- E. Chemical Vapor Deposition (CVD)

ABSTRACT

Mats of vertically-aligned multiwall carbon nanotubes were grown in an thermal CVD reactor with simultaneous feed of the catalyst and carbon precursors. Mats were soaked into epoxy resin solutions without any prior chemical modification and then cured to produce composite plates of z-axis nano-reinforcement. Direct observations of the epoxy–CNT interactions at the nanoscale revealed that epoxy interacted naturally with the MWCNTs without affecting their physical characteristics, alignment, or the mat's morphology. The compressive behavior of the pristine and composite mats was consistent with mechanical predictions accounting for an elastic regime followed by elastic instability and compaction. Strong evidence of reinforcement in the MWCNT/epoxy composites was indicated by increased strength, stiffness and toughness values with respect to the as-grown mats and pure polymer. The elastic instability strain of the composites was of the order of 0.4.

© 2012 Elsevier Ltd. All rights reserved.

1. Introduction

Owing to their unique physical properties, Carbon Nanotubes (CNTs) [1] are today the single most promising 1D material system for nanotechnology, optical, electronic and composite materials applications. Of particular interest to the material scientist is the development of new composite materials due to the extraordinary strengths achieved by both single- and multi-wall carbon nanotubes (SWCNTs and MWCNTs) [2] as well as their high toughness and unfamiliarly high aspect ratios [3]. The combination of such properties attracted the attention of the material science community that, soon after the first massive growth of carbon nanotubes in 1998 [4], foresaw the potential of the strong, tough and light tubes as reinforcing media for composite materials. The ideal type of nano-reinforcement would be long, continuous and well inter-aligned carbon nanotubes.

Advances in CNT growth techniques led to considerable increases in both production rate and product volume over the last years. Chemical Vapor Deposition (CVD) and its variants (plasma-enhanced-, vacuum-assisted-, aerosol-, catalytic-, etc.) is established as the most promising technique for large-scale production of CNTs [5,6]. Various research groups have grown vertically aligned carbon nanotubes on silicon and other substrates via CVD and have studied their compressive behavior [7–10]. Of particular

interest is the CVD route that uses camphor as carbon precursor [11–14] because camphor is an economical and environmentally-friendly chemical that conforms to the 12 principles of green chemistry as issued by the United States Environmental Protection Agency (US EPA). Despite the poor dispersibility of CNTs in polymeric matrices [15], attempts have also been made to infiltrate such aligned CNT arrays with polymers, for use in thermal management, conductive probes and field emission applications [16–18]. Indirect methods for homogeneously dispersing CNTs in polymeric media have also been reported [19–23] together with electric field [24], magnetic field [25,26], electrospinning [27] and mechanical force [21,28] methods of aligning nanotubes for the production of polymer nanocomposites of custom isotropies. The majority of these studies employs the chemical oxidation/modification route to increase the affinity of the graphitic surface with the polymer; a route that may, under certain conditions, have negative side-effects on the tubes' physical, thermal and electrical properties [29–31]. Wardle et al. have exploited the CNT-polymer capillary forces to successfully wet CNT forests by epoxy matrices via a submersion process without prior functionalization of the tubes [32,33]. According to their reports, they were able to control the only side-effect of the submersion method, namely CNT contraction due to the capillary forces; a process that can affect the shape of the nanocomposite microstructures. Very limited information is also available on the compressive properties of such vertically-aligned CNT nanocomposites [34–36]. Garcia et al. reported a 220% increase in the modulus of a CNT/thermoset–epoxy matrix with respect to the dry product [36] while Ci et al. claimed a

* Corresponding author at: Department of Materials Science and Engineering, University of Ioannina, Ioannina 45110, Greece.

E-mail address: kdassios@cc.uoi.gr (K.G. Dassios).

corresponding 3300% increase in a polydimethylsiloxane–matrix nanocomposite [35]. Robust and straightforward methodologies are still being sought for producing and characterizing polymer–CNT nanocomposites while (a) maintaining the tubes' orientation and alignment, and (b) diminishing the effects of processing parameters to the end product.

In the current study, we report on the manufacturing and compressive properties of epoxy-matrix nanocomposite plates reinforced by vertically-aligned, millimeter-high CNTs. The composites were achieved by direct impregnation of self-standing CVD-grown mats with epoxy resin. Possible applications of such nanocomposite mats include sandwich panel elements, electrochemical energy storage media, vibration absorbers, multifunctional and conductive composites applications. The proposed methodology involves a number of experimental steps including: (a) growth of thick mats of aligned MWCNTs in a thermal CVD reactor, (b) non-destructive separation of the mat from the substrate, (c) infiltrating the mats with resin by soaking in acetone solutions of uncured epoxy and (d) curing the impregnated mat to the resin-specific thermal cycle. The mechanical performance of the nanocomposite mats was studied in comparison to that of the as-grown CNT material.

2. Experimental

2.1. Growth of CNTs

The CVD procedure used in the current study is of particular interest because the catalyst precursor is fed into the system in a gas mixture in line with the carbon precursor; a method that eliminates the need of catalyst-coated surfaces. That way, MWCNTs can be grown on bare silicon substrates, on unconventional substrates such as Pyrex or quartz glass, even on curved substrates [37]. Another advantage of the continuous feed concept is that fresh catalyst particles are constantly introduced into the reactor to help maintain carbon precursor decomposition – hence also growth-active for prolonged periods of time. For this reason, the specific technique is known to be associated with growth of significantly thick CNT mats.

In the current study, mats of vertically aligned MWCNTs are grown in a horizontal quartz tube (1200 mm length, 40 mm diameter) that rests in a three-zone split-type tubular furnace. The tube is supplied with a constant nitrogen gas feed that maintains the system at a pressure just above atmospheric. The pulverized solid precursors, ferrocene (catalyst) and commercial camphor (carbon source), were mixed in a 1:20 ratio and transferred in a flask resting on a heater plate that is used to evaporate the mixture at 230 °C. The vapor mixture was introduced into the system by means of a T-join and was carried into the tube by the inert gas flux (Fig. 1). All parts of the setup between the heated flask and furnace inlet were kept at 230–240 °C by means of electrical heating bands to avoid local condensation of the vapors. Deposition was carried out on crystalline silicon substrates (1-0-0). The width of substrates was kept within 38 ± 1.5 mm, close to the tube's inner diameter, while their length varied from 100 to 200 mm. Pyrolysis of gases at 850 °C led to the deposition of carbon nanotubes on the surface of the Si wafers. The gaseous output at the tube end was introduced into a fume hood where it was burnt under an open flame burner before being introduced to the environment. This step is important for a forthcoming industrial application since it allows to efficiently get rid of polycyclic aromatic hydrocarbons (PAHs), such as naphthalene and phenanthrene, produced during the deposition [38]. While this study does not claim to have overcome the environmental concerns of the CVD process, which are mainly the discharge of greenhouse gases such as methane and

toxic compounds such as benzene [39], to the authors' knowledge, this is the first CNT growth reactor to implement a purification/reduction of the output gases. It was thereafter also possible to maintain a constant deposition rate within the reactor by controlling the evaporation rate of the precursors so as to keep an even flame length, downstream. Typical growth times ranged from 45 to 90 min and growth was terminated by stopping precursor evaporation and switching off the furnace. Upon cooling to room temperature, a considerable deposit of MWCNTs was found on the substrates and thinner deposits of MWCNTs were found on the inner walls of the quartz tube. The net height of as-grown material (excluding the silicon wafer thickness) ranged between 1.5 and 2.5 mm depending on deposition time. Given a constant feed system, it appears that no particular limitation hinders production of thicker mats. The optimal growth rate observed was $0.7 \mu\text{m s}^{-1}$ for a 2.3 mm high mat. CNT mats were separated from the silicon substrates with the help of a razor blade for further examination, processing and testing.

As verified by temperature measurements performed independently using an industrial K-type thermocouple probe, temperature remained constant within the central 550 mm of the total heated length of the tube, which was 750 mm (temperature distribution depicted in Fig. 1). Additionally, by running consecutive depositions while changing the wafer location along the tube, it was observed that growth was maximum within the central 350 mm of the uniform temperature region. The effect can be attributed to laminar flow characteristics acting locally to form a zone of optimal deposition conditions (Zone II, Fig. 1). Deposition was much less in the remaining two zones at the entry and exit of the furnace (Zones I and III, Fig. 1), probably a result of not fully developed and turbulent flows, respectively.

2.2. Production of nanocomposites

The matrix material chosen for impregnating the grown mats was the industrial Epikote™ 828LVEL/Epicure F205 resin system (Resolution Europe BV, the Netherlands). We selected this popular among the composite community thermosetting resin for its viscosity, good mechanical properties and chemical resistance in the cured state, as well as its ease of handling. Epikote™ 828LVEL is a medium viscosity epoxy resin, produced from bisphenol A and epichlorohydrin and contains no diluent. At 25 °C, its viscosity ranges from 10.0 to 12.0 Pa s while its density is 1.16 kg/l [40]. Epicure F205 is a low viscosity, modified cycloaliphatic amine curing agent with a viscosity of 0.5–0.7 Pa s and a density of 1.04 kg/l at 25 °C [41].

A plausible method to impregnate the as-deposited material with epoxy resin avoiding the complexity and side effects of chemical functionalization of CNTs, was sought. Several unsuccessful attempts to impregnate the mats with the uncured matrix, including vacuum-assisted infusion under 9 bars of pressure in autoclave environment, proved the material to be highly unfriendly with the target matrix. An investigation of the wettability of the mats in different solvents, eventually proved that the highly hydrophobic as-grown material was particularly friendly to one specific solvent: acetone [42]. Mats floated on acetone would absorb the liquid and sink while releasing entrapped air in an effervescent manner. The established acetone-friendly characteristic was important because acetone is also a good solvent for the uncured epoxy resin. Thereafter, blocks of CNT mats were wet in acetone-thinned solutions of 10%, 30% and 50% b.w. of uncured epoxy that was prepared by mixing the curing agent and resin in a 58:100 weight ratio [40,41]. Prior to soaking, the mats were rinsed with an acetone flow to remove all excess carbon particles and surface debris. The mats were left to soak in the epoxy solutions for 1 h; all effervescing activity appeared to cease already after approximately 30 min into soaking. The mats were subsequently cured

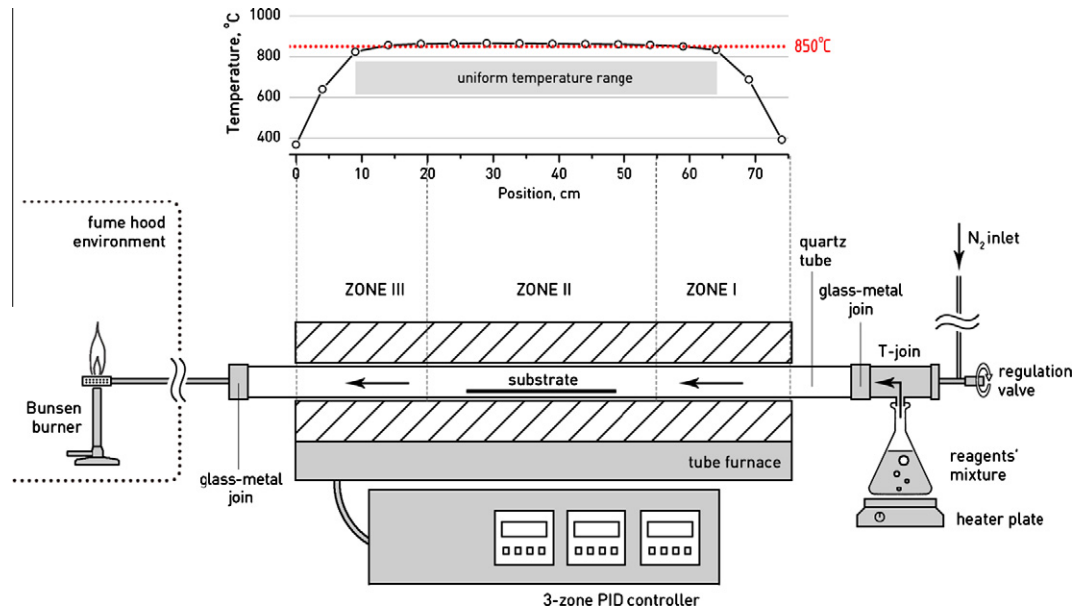


Fig. 1. Experimental setup for CVD growth of CNTs with simultaneous feed of carbon and catalyst precursors.

to the resin-specific cycle into a vacuum oven (Gallenkamp, Leicestershire UK); the cycle included a curing step at 80 °C for 2 h followed by post-curing at 130 °C for 1 h [40,41]. Upon cooling to room temperature, the impregnated mats were stiff enough to be straightforwardly cut into any right shape with a sectioning saw.

2.3. Specimens and testing

Compression specimens were prepared by cutting the impregnated mats into rectangular parallelepipeds of cross sectional areas of 15–20 mm² using a diamond wafering blade (Diamond Blade, Medium Grit, Medium Concentration, Ted Pella Inc., California, USA) on a low-speed precision sectioning saw (Buehler Isomet Low Speed Saw, Buehler Ltd., Illinois, USA). The height of the resulting composite plates remained equal to the as-grown value, 1.5–2.5 mm. Similar specimens were also prepared for the pristine material by sectioning the pure CNT mats with a razor blade. The cross sectional area of the latter specimens was approximately 25 mm².

To establish the compressive behavior of the matrix material independently, samples of pure epoxy were prepared by casting a 58:100 weight mixture of Epikure agent and Epikote resin in a Teflon assemblage providing an internal block volume of 20 × 20 × 30 mm³. Vacuum was used to compact the mixture for a period of 15 min. The system was then cured to the resin-specific cycle, following a procedure identical to the impregnated mats. Pure resin slices of cross sectional areas of 75–85 mm² and heights of 2.3–2.4 mm (comparable to the composite mats) were cut from the block using the aforementioned sectioning equipment.

Specimens of pure resin, as-grown MWCNT mats and epoxy-impregnated nanocomposite mats were tested in compression in an Instron® 5900 Electromechanical testing frame (Instron Industrial Products, Pennsylvania, USA) equipped with a 100 kN load cell. Testing was performed in cross-head displacement control with a strain rate of 0.1 min⁻¹.

3. Results and discussion

After separation from the silicon substrate, the as-grown MWCNT mats were self-standing and of macroscopic dimensions;



Fig. 2. Typical dimensions of as-grown product used for the production of the nanocomposite mats.

a typical block of the pristine material is presented in Fig. 2. The microstructure of the mats was investigated by SEM. As seen in Fig. 3, growth of MWCNTs followed a predominant vertically oriented pattern (Fig. 3a) coupled with a certain degree of inter-CNT entanglement prominent in higher magnifications (Fig. 3b). This branching is responsible not only for the free-standing integrity of the mat, but also for its potential, under certain conditions, to be drawn and twist-spun into CNT yarns [43]. The diameters of MWCNTs in the as-grown material ranged from 30 to 70 nm whereas the density of the mats was calculated at 0.35 g cm⁻³. This value is higher than what has been previously established with similar experimental setups [44]. On the other hand, the obtained value is lower than the bibliographically reported range for MWCNTs, 2.3–2.6 g cm⁻³ [45], an observation suggesting an openly-packed material. The actual pore structure of the as-deposited mats was analyzed in a PoreMaster® 60 mercury porosimeter (Quantachrome Instruments, Florida, USA). The results (Fig. 4) were fitted with a trimodal log-normal distribution function (dashed-line). It was observed that 88% of the pores ranged around a mean value of 0.4 µm with a standard deviation of 0.34 µm while 9% and 3% of the pores were found at 17 µm and 170 µm respectively. Hence, in the major part of the volume, the distance between tubes of a mean diameter of 50 nm, is equal to 8 tube diameters. This finding is compatible with the morphology pictured in Fig. 3b and indicates that the MWCNTs were fairly isolated throughout the volume of the mat. We believe that this is important in view of (a) the well-documented difficulty of other methods to achieve similar CNT homogeneity and (b) of the uniformity required in the target composite system. It should be stressed that the CVD synthesis process does not allow the formation of agglomerations (a situation usually encountered in nanotube mixing techniques) as each nanotube

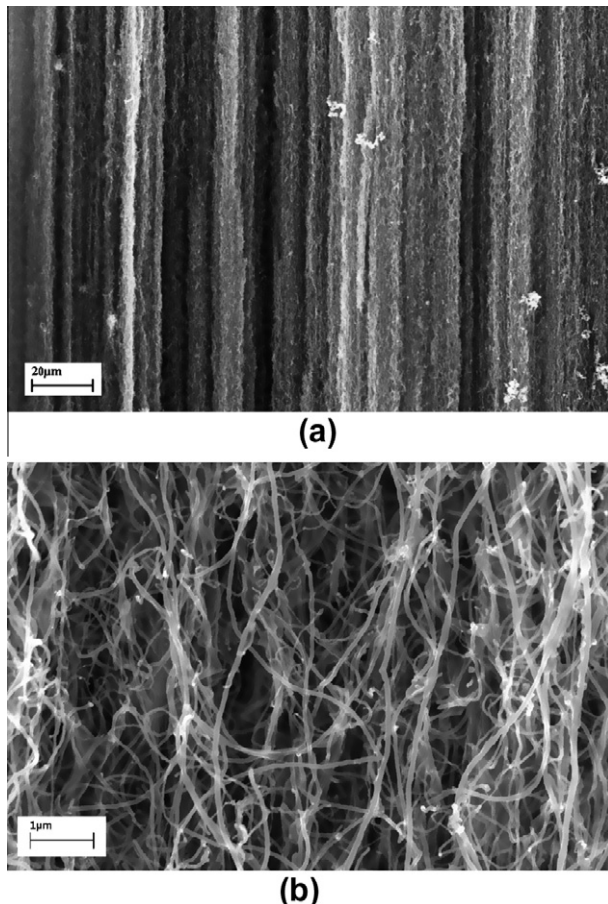


Fig. 3. SEM micrographs of the as-grown MWCNT mat. (a) Low magnification image demonstrating the dominant vertical arrangement of CNTs, and (b) branching observed between individual MWCNTs at higher magnifications.

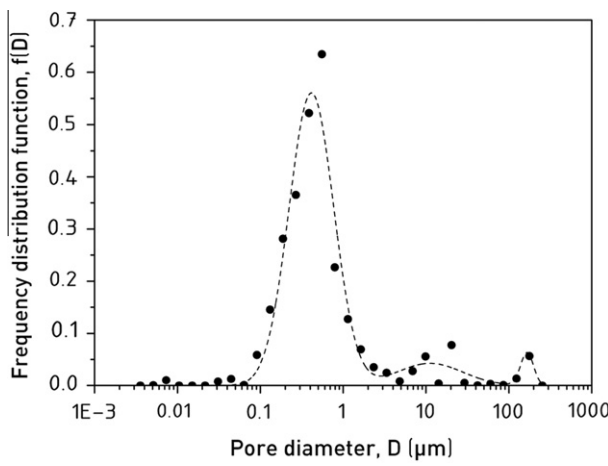


Fig. 4. Results of porosimetry measurements in the as-growth MWCNT mats.

grows separately in the vertical direction. The void fraction of the material was also established by porosimetry to be 0.73.

The void space coverage efficiency of the epoxy was examined under SEM by observation of cross-sections of composite mats soaked into solutions of varying resin concentration. Fig. 5a–c, demonstrates the topology of mats soaked in 10%, 30% and 50% b.w. solutions, respectively. In the thinner 10% and 30% solutions, epoxy was uniformly dispersed throughout the volume of the material and mixed well with the CNTs, forming, where available, well-defined

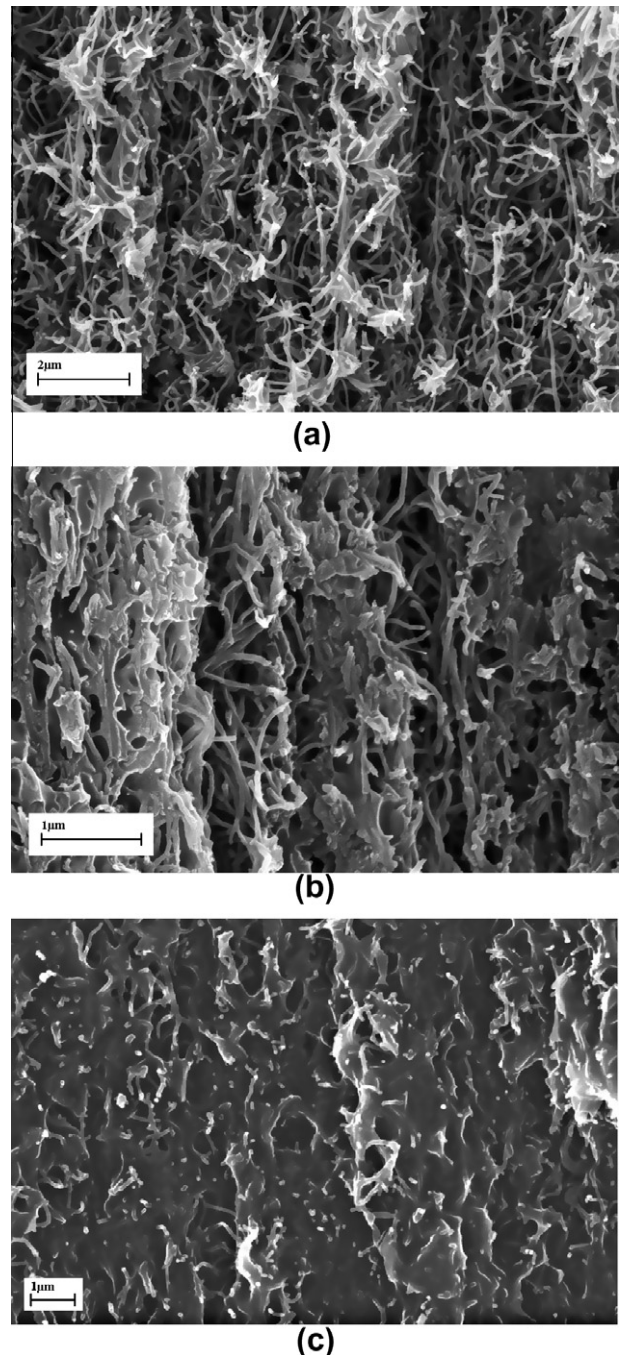


Fig. 5. SEM micrographs of sections of nanocomposite mats soaked in different concentrations of Epikote/Epikure epoxy showing the degree of resin coverage (a) 10%, (b) 30% and (c) 50% epoxy.

menisci between CNTs (Fig. 5a and b). However, it only provided partial coverage of the void space. As established by porosimetry, complete void coverage was achieved with the 50% by weight epoxy solution (Fig. 5c). Fig. 5 also demonstrates that the vertical orientation of CNTs in the mat remained unaffected by the interaction with the polymer and the thermal curing procedure. It appeared that epoxy interacted naturally with the acetone-soaked CNTs, a finding that contradicts a documented tendency of CNTs to aggregate in the presence of polymeric media [15].

The compressive behavior of the vertically-aligned-MWCNT/epoxy composites was compared to their as-grown counterparts. The calculation of stress for the pristine material took into account

the 0.27 CNT volume fraction obtained by porosimetry, whereas composite stress was calculated based on the total specimen cross section. The typical stress-strain behavior of pristine and composite mats is presented in Fig. 6a by the dashed and straight lines respectively, while the response of pure epoxy specimens is represented by a dotted line. The mechanical response of all three materials was consistent with the triple regime behavior (elastic/instable/plastic) expected by conventional mechanics for compression of identical beams entrapped between two parallel horizontal plates [44]. Therein, the elastic regime endures for axial loads up to the critical Eulerian buckling load for the beams, at which point elastic instability occurs, giving rise to a plastic contribution. The Euler load – hence also the stress of the beams – remains practically constant throughout the instability regime, which endures until the compaction mechanism commences, at the onset of the first nanotube fracture. This final regime is related with very steep stress-strain behavior, comparable to that of single tubes.

Instability in the epoxy resin occurred at ca. 12% strain – at which point the material had evidently failed – while compaction at ca. 50% strain. The corresponding values for the pristine and composite mats were identified in the plot of the first derivative of stress with respect to strain (Fig. 6b). It was thereby observed that both pristine and composite mats did not exhibit elastic instability up to 35% strain while nanotube fracture became significant at 75% and 60% strain for the pristine and composite materials respectively. By comparison it was noted that plasticity appears in the epoxy composite at three times higher strain than in the pure resin itself. Identifying the value of stress on the onset of com-

paction as the materials' strength for the given test configuration, we obtain values of 425 MPa and 1600 MPa for the as-grown and composite mats respectively. This 4-fold increase in strength indicates reinforcement.

The post mortem condition of the pristine and composite mats was examined by SEM and is shown in Figs. 7 and 8, respectively. As seen in Fig. 7a, the failed as-grown mats, which macroscopically appeared pulverized, were in a highly disorganized state consisting of randomly oriented short fragments of carbon nanotubes. The average intact length of the nanotubes was measured at 100–800 nm, while in many cases a carbon core was visible protruding around failed outer graphitic walls (Fig. 7b). The smallest core diameter was measured at ca. 8 nm. The post mortem appearance of the composites was impressive: contrary to the pristine material, the epoxy-filled mats retained their integrity up to 95% strain and were macroscopically self-standing after unloading at the end of the test. SEM imaging of the failed composite specimens revealed that extensive buckling of blocks of nanotubes had occurred during testing (Fig. 8a) and that cracks had formed and propagated perpendicular to the loading direction (Fig. 8a and b). The type of crack propagation, without crack deflection or delamination at the nanotube–matrix interphase, was compatible with a brittle material behavior and a strong CNT–epoxy bonding.

The pure polymer showed a typical linear behavior up to 12% strain, consistent with a modulus of 1.2 GPa and a failure strength of 90 MPa. The as-grown CNT mats exhibited quite low Young's moduli of ca. 80 MPa, which are considerably higher than previously

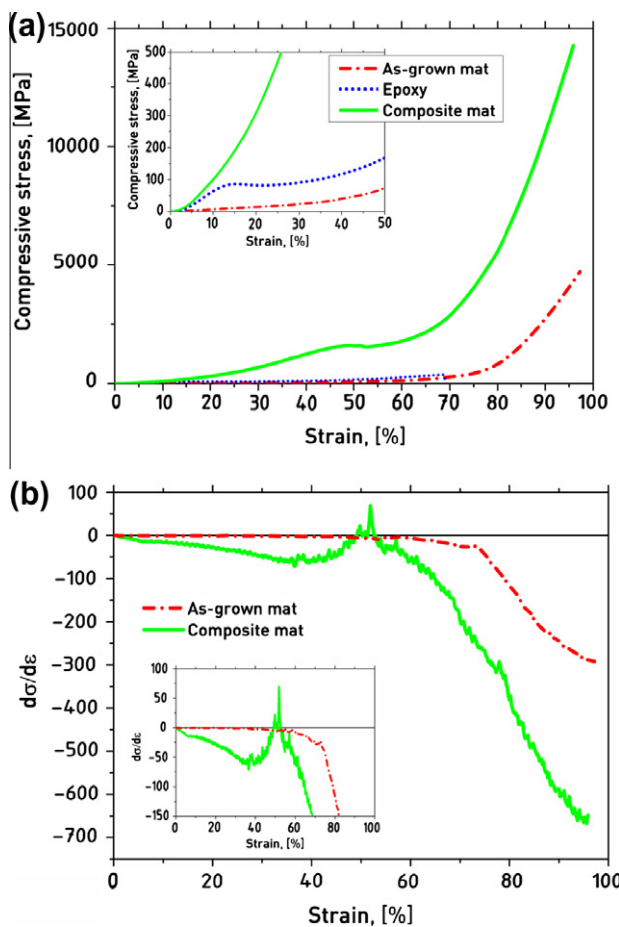


Fig. 6. Compressive behavior of as-grown and nanocomposite mats, as well as of the epoxy matrix. (a) Stress–strain curve, and (b) differential curve for damage regime allocation.

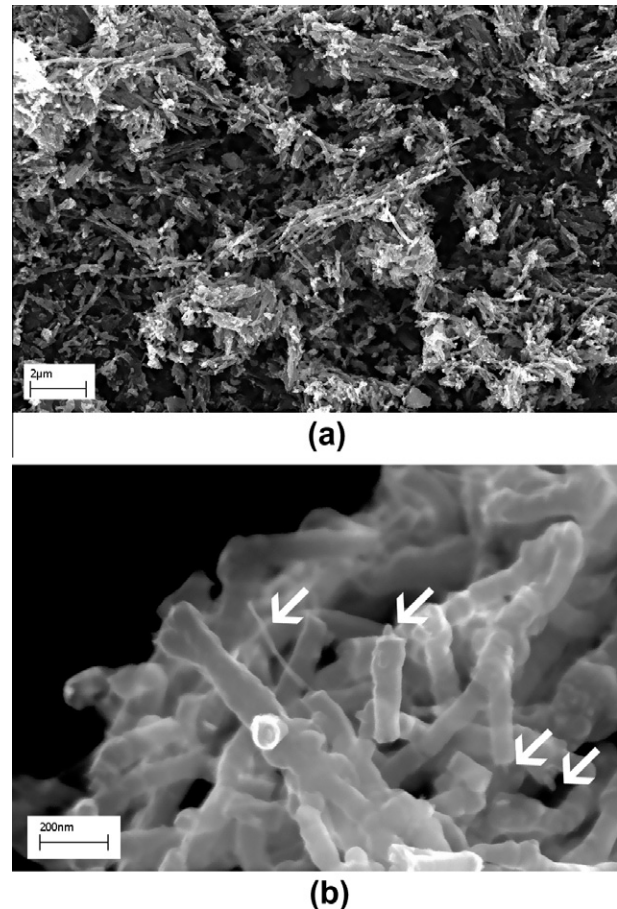


Fig. 7. SEM images of as-grown CNT mats failed under compression. (a) Low magnification image illustrating the randomly oriented tubes in the pulverized mass and (b) high magnification image illustrating typical intact length of tubes and CNT cores (indicated by arrows) protruding around failed graphitic walls.

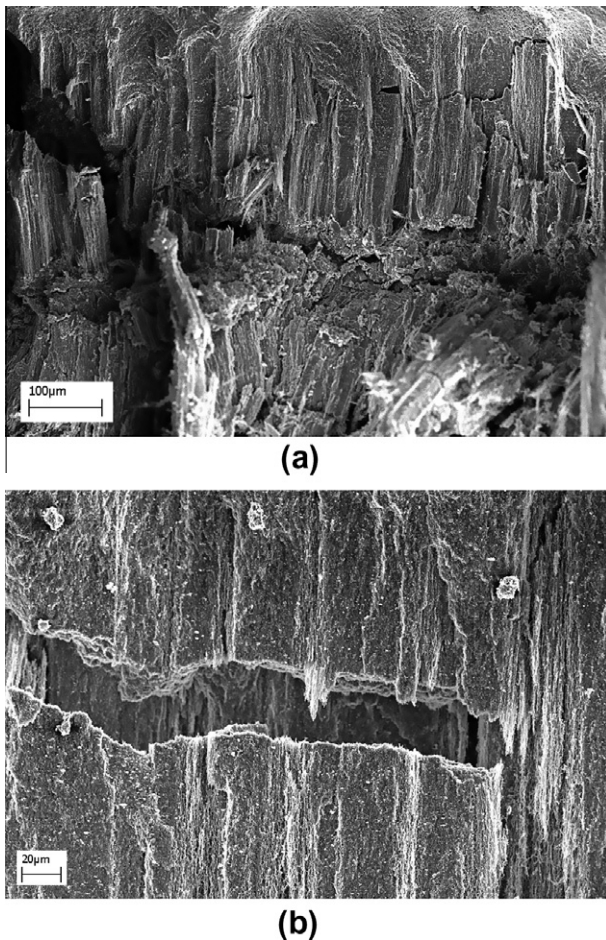


Fig. 8. SEM images of the thickness direction of failed composite mats. (a) Cracks formation normal to the loading direction and extensive buckling and (b) crack face separation during unloading.

quoted values of 0.25 MPa [46] and 4.5 MPa [47] for similar materials under compression. The corresponding modulus for the composite mat was 1.5 GPa, approximately 25% higher than the pure polymer modulus and 1800% higher than the as-grown mats' modulus. To comprehend the elastic performance of the mats under compression, we consider first a fundamental buckling model consisting of an array of identical, vertically-aligned beams of length L and elastic modulus E , compressed under constant stress between two parallel horizontal plates. The compressive modulus E_{compr} of this system can be approximated [46], for low strains, as:

$$E_{compr} = \frac{\pi^2 EI}{8AL^2} \quad (1)$$

where A is the average cross-sectional area of one tube and I the tube's area moment of inertia calculated as $I = \pi(D^4 - d^4)/64$ where D and d are the tube's outer and inner diameter, respectively. Inserting two extreme values of E established for CVD-grown MWCNTs, 12 GPa and 50 GPa [48], the mean outer and inner diameters of $D = 50$ nm and $d = 8$ nm measured herein by SEM, E_{compr} is found to range between 0.6 and 2.7 Pa for a 2 mm-high mat. The established range is four orders of magnitude lower than the as-grown dry mats and six orders of magnitude less than the experimentally measured composite modulus. Hence it is clear that the above analysis yields values much lower than both the values of as-grown dry CNT mats in air but also the impregnated (composite) CNT mats. The reason for that is that in both cases significant stress transfer occurs which provides resistance to bending and buckling, therefore, the

column buckling analysis is not appropriate. For example, in the case of the as-grown dry CNT mats the stress transfer occurs by the mechanical contact between CNTs (Fig. 3b) similar to entanglements between adjacent chains in polymers, whereas in the case of the impregnated mats, stress transfer and additional resistance to buckling is provided by the intervening polymer matrix. Schadler et al. have also discussed the relation between nanotube buckling and composite stiffness [49].

For the case of the composite mats, it is worth considering the conventional rule-of-mixtures using a nanotube volume fraction of $V_f = 0.27$:

$$E_{composite} = \Phi E_{MWCNT} V_f + E_m (1 - V_f) \quad (2)$$

where as mentioned earlier, $E_{MWCNT} = 12\text{--}50$ GPa, $E_m = 1.2$ GPa and Φ is the efficiency parameter that accounts for partial reinforcement due to discontinuous length of fibers and misorientation vis-à-vis the stress direction [50]. Using Eq. (2) and assuming $\Phi = 1$, a composite modulus in the range of 4–14 GPa is calculated. The experimental value corresponds to 10–38% of the calculated modulus which indicates that $\Phi < 1$. Given our previous findings of (a) fairly isolated filler dispersion and (b) low void content in the matrix, then the deviation from the conventional rule-of-mixtures ($\Phi = 1$) should be mainly due to CNT misalignment and the short length of the individual nanotubes. Other parameters that can affect the value of Φ are the interface strength and the presence of residual stresses [51]. Evidence has already been provided that the fabrication procedure mentioned earlier can ensure minimal residual stresses in the composite and that the interface is of reasonable strength as very limited pull-out is observed (see Fig. 5). However it is worth adding here that the interface strength is particularly important in compression as it affects significantly the buckling resistance of the composite. One way to increase the reinforcement efficiency index, Φ , of CNT forests is to modify chemically the CNT mat so as to reduce the effective length required for reinforcement. Possible routes for oxidative treatment of nanotubes is either washing the as grown mat with an acidic solution [52] or by prior plasma treatment. Both methods are currently in progress and will be reported in a future publication.

4. Conclusions

Millimeter-thick mats of vertically-aligned multiwall carbon nanotubes were grown via the thermal CVD route on silicon substrates in a tubular reactor with simultaneous feed of the catalyst-ferrocene, and carbon precursor-camphor, an environmentally-friendly product complying with the principles of Green Chemistry. The gaseous output of the reactor, containing PAHs, was purified by full oxidation under open flame before being released to the environment. A viable method for impregnating whole blocks of the highly hydrophobic as-grown material with epoxy resin was established by soaking the mats into acetone solutions of the uncured polymer. The soaked mats were cured to the resin-specific cycle to produce the final composite mats. The porosity of the as-deposited material was measured at 73% while the amount of void space decreased with increasing epoxy concentration in the soaking solution. SEM imaging indicated that CNTs did not aggregate in the presence of the epoxy, which appeared to diffuse naturally among the nanotubes. The morphology of the mats and vertical alignment of the tubes was retained in cured specimens. In accordance with theoretical predictions, a triple-regime mechanical behavior including elastic behavior, instability and compaction was observed for the as-grown and composite mats as well as the pure epoxy. The classical column buckling theory was not found appropriate to explain the experimental results that were approached satisfactorily through a rule-of-mixtures analysis. The

findings of 20-fold increase in Young's modulus and 4-fold increase in the strength of the composite with respect to the as-grown case, clearly indicated the effect of reinforcement in compression for the MWCNT/epoxy mats studied here.

References

- [1] Iijima S. Helical microtubules of graphitic carbon. *Nature* 1991;354(6348):56–8.
- [2] Li YJ, Wang KL, Wei JQ, Gu ZY, Wang ZC, Luo JB, et al. Tensile properties of long aligned double-walled carbon nanotube strands. *Carbon* 2005;43(1):31–5.
- [3] Zheng LX, O'Connell MJ, Doorn SK, Liao XZ, Zhao YH, Akhadov EA, et al. Ultralong single-wall carbon nanotubes. *Nat Mater* 2004;3(10):673–6.
- [4] Pan ZW, Xie SS, Chang BH, Wang CY, Lu L, Liu W, et al. Very long carbon nanotubes. *Nature* 1998;394(6694):631–2.
- [5] Hata K, Futaba DN, Mizuno K, Namai T, Yumura M, Iijima S. Water-assisted highly efficient synthesis of impurity-free single-walled carbon nanotubes. *Abstr Pap Am Chem S* 2005;229. U967–U967.
- [6] Pinault M, Pichot V, Khodja H, Launois P, Reynaud C, Mayne-L'Hermite M. Evidence of sequential lift in growth of aligned multiwalled carbon nanotube multilayers. *Nano Lett* 2005;5(12):2394–8.
- [7] Cao AY, Dickrell PL, Sawyer WG, Ghasemi-Nejhad MN, Ajayan PM. Super-compressible foamlke carbon nanotube films. *Science* 2005;310(5752):1307–10.
- [8] Deck CP, Flowers J, McKee GSB, Vecchio K. Mechanical behavior of ultralong multiwalled carbon nanotube mats. *J Appl Phys* 2007;101(2).
- [9] Zbib AA, Mesarovic SD, Lilleodden ET, McClain D, Jiao J, Bahr DF. The coordinated buckling of carbon nanotube tufts under uniform compression. *Nanotechnology* 2008;19(17).
- [10] Misra A, Greer JR, Daraio C. Strain rate effects in the mechanical response of polymer-anchored carbon nanotube foams. *Adv Mater* 2009;21(3):334–8.
- [11] Kumar M, Ando Y. A simple method of producing aligned carbon nanotubes from an unconventional precursor – camphor. *Chem Phys Lett* 2003;374(5–6):521–6.
- [12] Kumar M, Ando Y. Single-wall and multi-wall carbon nanotubes from camphor – a botanical hydrocarbon. *Diam Relat Mater* 2003;12(10–11):1845–50.
- [13] Mukul Kumar YA. Carbon Nanotubes from Camphor: An Environment-Friendly Nanotechnology. *J Phys: Conf Ser* 2007;61:643. <http://dx.doi.org/10.1088/1742-6596/61/1/129>.
- [14] Porro S, Musso S, Giorcelli M, Chiodoni A, Tagliaferro A. Optimization of a thermal-CVD system for carbon nanotube growth. *Physica E* 2007;37(1–2):16–20.
- [15] Lau KT, Hui D. Effectiveness of using carbon nanotubes as nano-reinforcements for advanced composite structures. *Carbon* 2002;40(9):1605–6.
- [16] Huang H, Liu CH, Wu Y, Fan SS. Aligned carbon nanotube composite films for thermal management. *Adv Mater* 2005;17(13). 1652–+.
- [17] Jung YJ, Kar S, Talapatra S, Soldano C, Viswanathan G, Li XS, et al. Aligned carbon nanotube-polymer hybrid architectures for diverse flexible electronic applications. *Nano Lett* 2006;6(3):413–8.
- [18] Yaglioglu O, Martens R, Hart AJ, Slocum AH. Conductive carbon nanotube composite microprobes. *Adv Mater* 2008;20(2). 357–+.
- [19] Barrera EV. Key methods for developing single-wall nanotube composites. *Jom-J Miner Met Mater Soc* 2000;52(11):A38–42.
- [20] Schadler LS, Giannaris SC, Ajayan PM. Load transfer in carbon nanotube epoxy composites. *Appl Phys Lett* 1998;73(26):3842–4.
- [21] Jin L, Bower C, Zhou O. Alignment of carbon nanotubes in a polymer matrix by mechanical stretching. *Appl Phys Lett* 1998;73(9):1197–9.
- [22] Yang K, Gu MY, Guo YP, Pan XF, Mu GH. Effects of carbon nanotube functionalization on the mechanical and thermal properties of epoxy composites. *Carbon* 2009;47(7):1723–37.
- [23] Liu W, Zhang XH, Xu G, Bradford PD, Wang X, Zhao HB, et al. Producing superior composites by winding carbon nanotubes onto a mandrel under a poly(vinyl alcohol) spray. *Carbon* 2011;49(14):4786–91.
- [24] Zhu YF, Ma C, Zhang W, Zhang RP, Koratkar N, Liang J. Alignment of multiwalled carbon nanotubes in bulk epoxy composites via electric field. *J Appl Phys* 2009;105(5).
- [25] Kimura T, Ago H, Tobita M, Ohshima S, Kyotani M, Yumura M. Polymer composites of carbon nanotubes aligned by a magnetic field. *Adv Mater* 2002;14(19):1380–3.
- [26] Chiolerio A, Musso S, Sangermano M, Giorcelli M, Bianco S, Coisson M, et al. Preparation of polymer-based composite with magnetic anisotropy by oriented carbon nanotube dispersion. *Diam Relat Mater* 2008;17(7–10):1590–5.
- [27] Sen R, Zhao B, Perea D, Iltks ME, Hu H, Love J, et al. Preparation of single-walled carbon nanotube reinforced polystyrene and polyurethane nanofibers and membranes by electrospinning. *Nano Lett* 2004;4(3):459–64.
- [28] Vigolo B, Penicaud A, Coulon C, Sauder C, Pailler R, Journet C, et al. Macroscopic fibers and ribbons of oriented carbon nanotubes. *Science* 2000;290(5495):1331–4.
- [29] Zhang J, Zou HL, Qing Q, Yang YL, Li QW, Liu ZF, et al. Effect of chemical oxidation on the structure of single-walled carbon nanotubes. *J Phys Chem B* 2003;107(16):3712–8.
- [30] Liu CH, Fan SS. Effects of chemical modifications on the thermal conductivity of carbon nanotube composites. *Appl Phys Lett* 2005;86(12).
- [31] Garg A, Sinnott SB. Effect of chemical functionalization on the mechanical properties of carbon nanotubes. *Chem Phys Lett* 1998;295(4):273–8.
- [32] Wardle BL, Saito DS, Garcia Ej, Hart AJ, de Villoria RG, Verploegen EA. Fabrication and characterization of ultrahigh-volume-fraction aligned carbon nanotube-polymer composites. *Adv Mater* 2008;20(14). 2707–+.
- [33] Garcia Ej, Hart AJ, Wardle BL, Slocum AH. Fabrication of composite microstructures by capillarity-driven wetting of aligned carbon nanotubes with polymers. *Nanotechnology* 2007;18(16).
- [34] Thostenson ET, Chou TW. On the elastic properties of carbon nanotube-based composites: modelling and characterization. *J Phys D Appl Phys* 2003;36(5):573–82.
- [35] Ci L, Suhr J, Pushparaj V, Zhang X, Ajayan PM. Continuous carbon nanotube reinforced composites. *Nano Lett* 2008;8(9):2762–6.
- [36] Garcia Ej, Hart AJ, Wardle BL, Slocum AH. Fabrication and nanocompression testing of aligned carbon-nanotube-polymer nanocomposites. *Adv Mater* 2007;19(16). 2151–+.
- [37] Musso S, Fanchini G, Tagliaferro A. Growth of vertically aligned carbon nanotubes by CVD by evaporation of carbon precursors. *Diam Relat Mater* 2005;14(3–7):784–9.
- [38] Musso S, Zanetti M, Giorcelli M, Tagliaferro A, Costa L. Gas chromatography study of reagent degradation during chemical vapor deposition of carbon nanotubes. *J Nanosci Nanotechnol* 2009;9(6):3593–8.
- [39] Plata DL, Hart AJ, Reddy CM, Gschwend PM. Early evaluation of potential environmental impacts of carbon nanotube synthesis by chemical vapor deposition. *Environ Sci Technol* 2009;43(21):8367–73.
- [40] Epikote 828 L VEL Product Data Sheet. EK 1.1.81. Resolution performance products; 2002.
- [41] Epikure F205 Product Data Sheet. EK 1.4.18. Resolution performance products; 2001.
- [42] Dassios K, Galiotis C. Polymer–nanotube interaction in MWCNT/poly(vinyl alcohol) composite mats, submitted for publication.
- [43] Zhang M, Atkinson KR, Baughman RH. Multifunctional carbon nanotube yarns by downsizing an ancient technology. *Science* 2004;306(5700):1358–61.
- [44] Pavese M, Musso S, Pugno NM. Compression behaviour of thick vertically aligned carbon nanotube blocks. *J Nanosci Nanotechnol* 2010;10(7):4240–5.
- [45] Qi HJ, Teo KBK, Lau KKS, Boyce MC, Milne WI, Robertson J, et al. Determination of mechanical properties of carbon nanotubes and vertically aligned carbon nanotube forests using nanoindentation. *J Mech Phys Solids* 2003;51(11–12):2213–37.
- [46] Tong T, Zhao Y, Delzeit L, Kashani A, Meyyappan M, Majumdar A. Height independent compressive modulus of vertically aligned carbon nanotube arrays. *Nano Lett* 2008;8(2):511–5.
- [47] Musso S, Giorcelli M, Pavese M, Bianco S, Rovere M, Tagliaferro A. Improving macroscopic physical and mechanical properties of thick layers of aligned multiwall carbon nanotubes by annealing treatment. *Diam Relat Mater* 2008;17(4–5):542–7.
- [48] Salvetat JP, Kulik AJ, Bonard JM, Briggs GAD, Stockli T, Metenier K, et al. Elastic modulus of ordered and disordered multiwalled carbon nanotubes. *Adv Mater* 1999;11(2):161–5.
- [49] Ravarikar NR, Vijayaraghavan AS, Keblinski P, Schadler LS, Ajayan PM. Embedded carbon-nanotube-stiffened polymer surfaces. *Small* 2005;1(3):317–20.
- [50] Krenchel H. Fibre reinforcement. Copenhagen: Alademisk forlag; 1964.
- [51] Filiou C, Galiotis C, Batchelder DN. Residual-stress distribution in carbon-fiber thermoplastic matrix preimpregnated composite tapes. *Composites* 1992;23(1):28–38.
- [52] Datsyuk V, Kalyva M, Papageorgis K, Parthenios J, Tasis D, Siokou A, et al. Chemical oxidation of multiwalled carbon nanotubes. *Carbon* 2008;46(6):833–40.